Functional Incorporation of Integrins into Solid Supported Membranes on Ultrathin Films of Cellulose: Impact on Adhesion

Stefanie Goennenwein,* Motomu Tanaka,* Bin Hu,† Luis Moroder,‡ and Erich Sackmann*
*Technische Universität München, Garching, Germany; †Lerner Research Institute, The Cleveland Clinic Foundation, Cleveland, Ohio 44195; USA; and ‡Max Planck Institut für Biochemie, Martinsried, Germany

ABSTRACT Biomimetic models of cell surfaces were designed to study the physical basis of cell adhesion. Vesicles bearing reconstituted blood platelet integrin receptors $\alpha_{IIb}\beta_3$ were spread on ultrathin films of cellulose, forming continuous supported membranes. One fraction of the integrin receptors, which were facing their extracellular domain toward the aqueous phase, were mobile, exhibiting a diffusion constant of 0.6 $\mu m^2\ s^{-1}$. The functionality of receptors on bare glass and on cellulose cushions was compared by measuring adhesion strength to giant vesicles. The vesicles contained lipid-coupled cyclic hexapeptides that are specifically recognized by integrin $\alpha_{IIb}\beta_3$. To mimic the steric repulsion forces of the cell glycocalix, lipids with polyethylene glycol headgroups were incorporated into the vesicles. The free adhesion energy per unit area Δg_{ad} was determined by micro-interferometric analysis of the vesicle's contour near the membrane surface in terms of the equilibrium of the elastic forces. By accounting for the reduction of the adhesion strength by the repellers and from measuring the density of receptors one could estimate the specific receptor ligand binding energy. We estimate the receptor-ligand binding energy to be 10 k_BT under bioanalogue conditions.

INTRODUCTION

Solid supported lipid membranes with functional proteins have been intensively and widely investigated in the last decades as a general model of cell membranes (Sackmann, 1996). They have been used especially for the study of cell adhesion (Chan et al., 1991, Dustin, 1997, Bruinsma et al., 2000) or protein interactions (Brian and McConnell, 1984) as well as for the design of biosensors on electrical devices (Hillebrandt et al., 1999). One advantage of planar membranes is the possibility to study structural and dynamical properties by numerous surface sensitive techniques (Watts et al., 1986, Salafsky et al., 1996, Wong et al., 1999). A commonly used method to reconstitute proteins into supported bilayers is to incorporate them into lipid vesicles and spread these proteoliposomes onto solid surfaces (Kalb et al., 1992). Membrane-spanning proteins such as ion channels or bacteriorhodopsins (Puu et al., 2000) can be reconstituted into supported membranes which are in contact with solid surfaces without a considerable reduction of their function. However, for cell-adhesion studies the situation is more complicated, since the functional headgroups of the receptors are very large and can stick out of the membrane up to several 10 nm (Sackmann and Bruinsma, 2002). Since the distance between membranes and solid substrates is typically smaller than 1 nm, the large headgroups touch the solid substrates, which often results in the denaturation of the proteins. One strategy to overcome this problem is to separate the bilayer from the solid support either by incorporation of lipopolymers into the membrane (Heyse et al., 1995) or by coating the surface with soft, ultrathin biocompatible polymer ''cushions'' (Wegner, 1993). As demonstrated previously, pure lipid bilayers can be spread homogeneously on cellulose cushions (Sigl et al., 1997). Recently, even the homogeneous and orientation-selective immobilization of human erythrocyte membranes on these cellulose films was accomplished (Tanaka et al., 2001).

Integrin $\alpha_{IIb}\beta_3$ receptors are cell-adhesion molecules, which are expressed on human blood platelets and play a critical role in thrombosis and hemostasis (Hynes, 1992). The integrin (depicted schematically in Fig. 1 *b*, molecular mass ~240 kDa) has a small intracellular domain and a large extracellular domain ($8 \times 12\ nm^2$ lateral dimensions), which bears a specific binding site for fibrinogen, fibronectin, von Willebrand's factor and vitronectin. Integrin $\alpha_{IIb}\beta_3$ binds specifically to Arg-Gly-Asp (RGD) sequences of these ligands. The receptors were reconstituted into lipid vesicles. These proteoliposomes were spread onto solid surfaces covered by multilayers of rodlike cellulose molecules (thickness $d \simeq 5\ nm$). The supported membranes exhibited a homogeneous coating over large areas ($18 \times 18\ mm^2$), enabling partially long-range lateral diffusion of reconstituted receptors pointing their extracellular domains into the aqueous phase. In contrast, the receptors are essentially immobile if the proteoliposomes were spread directly onto bare glass slides and a complete fusion of the membrane was impeded.

The functionality of the integrin receptors was tested quantitatively by measuring the free adhesion energy Δg_{ad} (also called spreading pressure) to giant vesicles. These vesicles bear lipid-coupled cyclic hexapeptides which contain the RGD sequence. Using the micro-interferometric technique (Albertsdörfer et al., 1997), the free adhesion energy can be determined from the vesicle's contour close to

Submitted October 25, 2002, and accepted for publication February 10, 2003.

Address reprint requests to Stefanie Goennenwein, Technische Universität München, James-Franck-Str. 1, D-85748 Garching, Germany. Tel.: 49-8928912470; Fax: 49-8928912469; E-mail: smarx@ph.tum.de.

0006-3495/03/07/646/10 $2.00

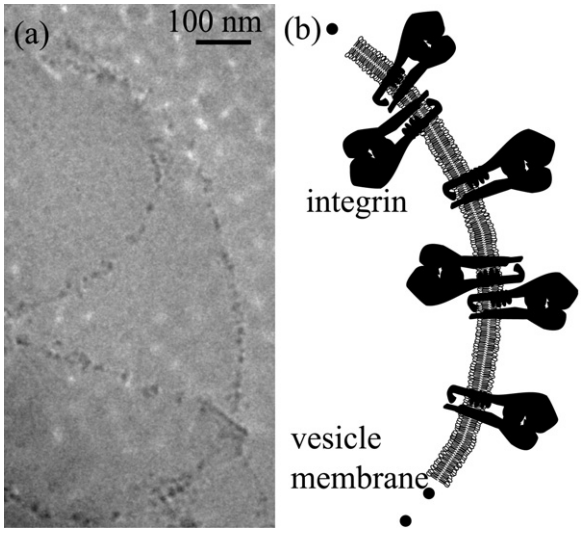

FIGURE 1 (*a*) Cryo-electron micrograph of reconstituted integrin $\alpha_{IIb}\beta_3$ receptors in DMPC/DMPG vesicles. The black protrusions in the vesicles membranes correspond to integrins. (*b*) Schematic illustration of the lipid vesicle containing integrin receptors, where the large extracellular parts are exposed on both sides of the membrane. The picture is drawn to scale.

the substrate. For vesicles adhering to bilayers supported on cellulose films, the measured spreading pressure Δg_{ad} agreed well with the value calculated from the density and the estimated binding constant of the receptors in the supported membrane.

Repeller molecules (lipids with polyethylene glycol headgroups) were incorporated into the giant vesicles to mimic the repulsive forces exerted by the glycocalix of the cell plasma membranes. These repeller molecules have been postulated to decrease the free adhesion energy Δg_{ad} due to the osmotic pressure difference $\Delta\pi_R$ between the adhering and the nonadhering parts of the membrane (Bruinsma et al., 2000). Indeed, an increase in the repeller concentration led to a decrease in the adhesion energy. By extrapolating the measured spreading pressure Δg_{ad} to zero repeller concentration we could estimate the specific adhesion energy W_{ad}. Surprisingly, the formation of tight adhesion domains was not accompanied by a pronounced lateral repeller segregation. We found only a small decrease of 3% for the repeller concentration in the tight adhesion domain. This result can be explained by the larger integrin headgroup (~12 nm) in comparison to the Flory radius of the repeller headgroup. The extrapolated specific adhesion energy W_{ad} and the measured receptor density enabled us to determine single receptor-ligand interaction energies under biocompatible conditions.

The major motivation for the present work was to measure forces between receptors and ligands in a biological environment. To this end a model system was established which allows for force measurements between receptor ligand pairs coupled to soft surfaces. Although the presented model system does not represent the true physiological situation where the RGD-bearing ligands are an integral part of the tissue surface (e.g. vitronectin) or form soluble linkers between cell membranes and tissues as the von Willebrand factor, it mimics well the physical situations of membrane adhesion. As demonstrated earlier such model systems are helpful to gain physical insights into the control of the adhesion processes, since the contributions of the various forces can be controlled (Albertsdörfer et al., 1997). In the supported bilayers the receptors pointing toward the substrate do not interfere with the adhesion process. However, they generate a structure very similar to cell plasma membranes, where the lipid/protein bilayer is spatially separated from the surface of the actin cortex. The membranes of giant vesicles are in a fluid state, which allows a rapid diffusion of the lipid coupled RGD ligands and corresponds to that of soluble van Willebrand factors.

MATERIALS AND METHODS

Cellulose

Glass coverslides were purchased from Merck (Germany) and used as substrates. They were rinsed by sonication in acetone and methanol, and immersed into 1:1:5 (v/v) solution of $H_2O_2/NH_4OH/H_2O$ at 60°C for 30 min. After rinsing extensively with ultrapure water (Millipore, France), the slides were dried at 70°C and stored in a vacuum chamber for at least 12 h. The substrates were immersed into a 5 vol % solution of octadecyltrimethoxysilane (ODTMS, ABCR, Karlsruhe, Germany) in dry toluene, adding 0.5 vol % butylamine as a catalyst (Mooney et al., 1996). The samples were sonicated for 60 min at a controlled temperature of 13°C, and soaked for another 30 min. To remove physisorbed ODTMS from the surface, the samples were then carefully rinsed and sonicated for 2 min in toluene.

Trimethylsilyl cellulose (TMSC) was synthesized as previously reported (Schaub et al., 1993). The degree of substitution (*DS*) was estimated by elemental analysis to $DS \sim 2.0$. Thin films of trimethylsilyl cellulose (TMSC) were deposited by Langmuir-Blodgett technique, where the lateral pressure was kept constant at 30 mN/m and a the subphase temperature was 17°C (Hillebrandt et al., 1999). The transferred films (10 layers, thickness ~10 nm) were dried in a vacuum chamber and exposed to a saturated vapor of concentrated HCl for 15–30 s in order to regenerate original cellulose by cleavage of silyl sidegroups (film thickness after regeneration ~5 nm).

Integrin $\alpha_{IIb}\beta_3$

Integrin $\alpha_{IIb}\beta_3$ was extracted by Triton-X 100 (Sigma-Aldrich, Germany) from outdated human blood platelets of the local blood bank (Fitzgerald et al., 1985). Function of the purified receptors was checked by enzyme-linked immunosorbent assay (ELISA) tests. For reconstitution into small vesicles Triton-X 100 was removed by Bio-Beads SM2 (Bio-Rad, Germany), as described previously (Müller et al., 1993, Hu et al., 2000). As matrix lipids we used a 1:1 mixture (by molar fraction) of DMPC and DMPG ((1,2-dimyristoyl-*sn*-glycero-3-phosphocholine and -phosphatidylglycerol), purchased from Avanti Polar Lipids Inc. (Alabaster, AL, USA). The integrin-containing vesicles were dialyzed to 150 mM NaCl, 20 mM TRIS, 1 mM NaN_3, 1 mM $CaCl_2$, 1 mM $MgCl_2$ at pH 7.3, called buffer *A* in the following.

For fluorescence experiments, integrins were labeled with 5-(and-6)-carboxy-tetra-methylrhodamine succinimidyl ester (5(6)-TAMRA-SE) purchased from Molecular Probes, Inc. (Eugene, OR, USA), as reported earlier (Hu et al., 2000). The labeling efficiency was measured to be 1:1 with spectroscopy. These labeled proteins were mixed with unlabeled ones, yielding a final molar fraction of labeled proteins of 0.1.

In order to label the lipid moiety of the vesicle membrane 1-oleoyl-2-[12-[(7-nitro-2-1,3-benzoxadiazol-4-yl)amino] dodecanoyl]-*sn*-glycero-3- phosphocholine (called NBD-PC in the following) purchased from Molecular Probes was added to pure lipids at a concentration of 1–2 mol %.

Synthesis of RGD ligand

The synthesis of cyclic RGD-peptide (c[Arg-Gly-Asp-D-Phe-Lys(NBD)-Gly-]) was reported by Gurrath et al., (1992) and the coupling of the RGD sequence to DMPE (1,2-dimyristoyl-*sn*-glycero-3-phosphoethanolamine) was reported elsewhere (Hu et al., 2000).

The fluorescently labeled RGD peptide was synthesized as follows: 6-(N-(7-Nitrobenz-2-oxa-1,3-diazol-4-yl)aminohexanoic acid (NBD) (18 mg; 62 μmol) was coupled to the cyclic peptide c[Arg(Pbf)-Gly-Asp(OtBu)-D-Phe-Lys-Gly-] (30 mg; 31 μmol) in 5 ml of freshly destilled DMF by HATU (24 mg; 62 μmol), HOAt (9 mg; 62 μmol) and DIPEA (17 μl; 120 μmol). After 4 h, the solvent was removed and the residue was taken up in ethyl acetate. The insoluble product was centrifuged and the solid was treated with 95% aqueous TFA containing 1.5% triethylsilane for 2 h. The crude product was purified batchwise by reversed phase HPLC on XTerra C18 (Waters, MA, USA) with a linear gradient of 5%–60% AcCN in 0.01% TFA in 45 min; yield: 7 mg (22%); HPLC: $t_r = 6.2$ min (Luna 150 × 4.6 5μ C18, phenomenex); ESI-MS: m/z = 969.4 [M+H$^+$] $M_r = 968.5$ calculated for $C_{46}H_{68}N_{10}O_{11}S$.

Supported planar bilayers

Supported planar bilayers were formed by direct fusion of integrin-loaded vesicles (Müller et al., 1993) onto bare glass slides and onto slides coated with cellulose films, respectively. The substrate formed the bottom of the measuring chamber, which was assembled by pressing a Teflon frame onto the substrate with the help of a metal frame. This measuring chamber was filled with 200 μl of the vesicle suspension and covered by a glass slide. After 2.5 h of incubation, the osmolarity of the solution was increased by 25 mOsm with respect to the intravesicular medium. After another hour of incubation, the sample was rinsed intensively with buffer *A* to remove physisorbed vesicles. For adhesion experiments, nonspecific binding was blocked by incubation with a 3 wt % solution of BSA in buffer *A* for 1 h. Finally, the sample was rinsed with buffer *A* to remove nonadsorbed material.

Giant vesicles

Giant vesicles were composed of an equimolar mixture of DMPC and cholesterol, 1 mol % of DMPE with polyethylene glycol headgroups (PEG lipid, molecular mass(PEG) = 2000) and 1 mol % of DMPE with a cyclic RGD peptide headgroup (RGD lipid, synthesized as described before), in respect to the DMPC amount were added. All components were purchased from Avanti. Giant vesicles were prepared by the electro-swelling technique (Dimitrov and Angelova, 1988, Albertsdörfer et al., 1997). For this purpose, lipids were dissolved in chloroform and deposited onto indium-tin-oxide electrodes. The swelling chamber was filled with 170 mM sucrose solution and the content was exposed to an AC electric field of 10 Hz and 1 A for 2 h. 200 μl of the obtained giant vesicle suspension was injected into the measuring chamber which contained buffer *B* (100 mM NaCl, 10 mM HEPES, 1 mM NaN_3, 1 mM $CaCl_2$ at pH 7.3 and 205 mOsm). The vesicles settled on the bottom of the measuring chamber due to the higher density of the intravesicular sucrose solution with respect to the outer buffer *B* ($\Delta\rho$ = 49.5 kg/m^3). Due to an osmotic pressure difference of 30–40 mOsm between the inner and outer medium of the vesicle, the vesicles were deflated. Thereby, excess area is generated, enabling vesicles to adhere to flat surfaces.

Fluorescence microscopy

The homogeneity and the lateral distribution of the labeled lipids and proteins were checked with an inverted microscope Axiovert 200 (Zeiss, Germany) equipped with a neofluar objective (antiflex, 63×, oil immersion, NA = 1.3). The dyes were excited with a high pressure mercury lamp combined with fluorescence filters that transmit at 540–550 nm for TAMRA and at 450–490 nm for NBD. Fluorescence emission was detected above 590 nm (TAMRA) or 515 nm (NBD), respectively, with a cooled 12 bit camera (Orca-ER, Hamamatsu, Japan). The data collection was carried out through a real-time imaging software developed at our laboratory.

Reflection interference contrast microscopy

Adhesion of giant vesicles was studied by a micro-interferometric technique, called reflection interference contrast microscopy (RICM) (Albertsdörfer et al., 1997). RICM images are formed by interference of light reflected from the interface glass buffer and the surface of the adhering vesicle, respectively. The contour of the adhering vesicle in the vicinity of the substrate could be reconstructed by an inverse cosine transformation.

Fluorescence recovery after photobleaching

The lateral mobility in the bilayer was measured by fluorescence recovery after photobleaching (FRAP) (Axelrod et al., 1976). The fluorescent labels were bleached within a circular spot of 9.3 μm diameter by a focused laser pulse of an Ar^+-Laser (Innova 70, Coherent, Santa Clara, CA, USA). Recovery of the fluorescence signal was monitored by a photomultiplier (RCA 31034-04). The lateral diffusion constant *D* was obtained by analyzing the fluorescence recovery according to the theoretical model of Soumpasis (1983), which holds for a rectangular intensity profile of the bleaching light.

RESULTS AND DISCUSSION

Determination of integrin and lipid concentrations in vesicles

The reconstitution of integrins into lipid vesicles was confirmed by electron micrographs of cryo-fixed samples. In the example of Fig. 1 *a*, the reconstituted $\alpha_{IIb}\beta_3$ receptors are visible as small protrusions extending from both sides of the vesicle membrane. Closer inspection of many samples showed that these protrusions have a quite regular length of ~20 nm, which is in good agreement with other studies (Erb et al., 1997). The receptors are rather evenly distributed over the vesicle surface. The protein concentration in the vesicles was determined by UV spectroscopy measurements, following the procedure reported by Bradford (1976). The lipid concentration was measured by phosphate analysis according to Fiske and SubbaRow (1925). We found an integrin concentration of 56 nM and a lipid concentration of 400 μM, corresponding to an integrin to lipid molar ratio of 1:7000. This protein content is rather high, although it is a factor of five smaller than the highest concentration reported, 1:1500 (Müller et al., 1993). The measured lipid to protein molar ratio corresponds to an average protein distance of 60 nm in the membrane.

Formation of planar membranes with integrins

Fig. 2 shows the fluorescence micrograph of a supported membrane with labeled integrins on a bare glass substrate.

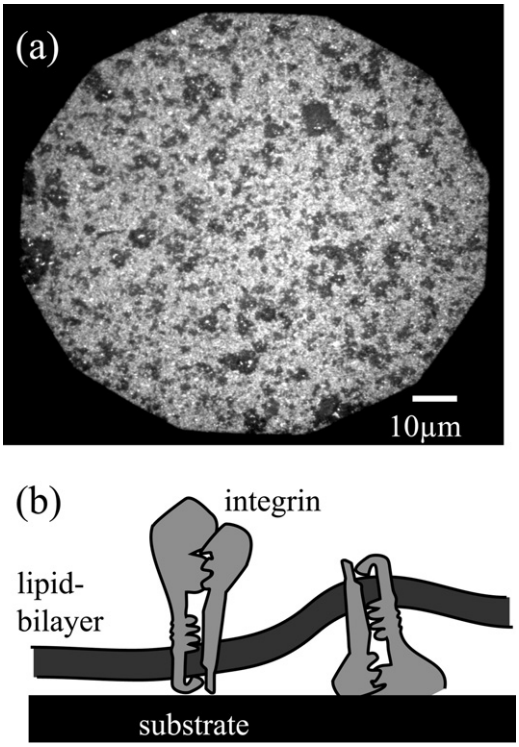

FIGURE 2 (*a*) Fluorescence micrograph of a membrane containing labeled integrins on a bare glass substrate. (*b*) Side view of the solid supported membrane.

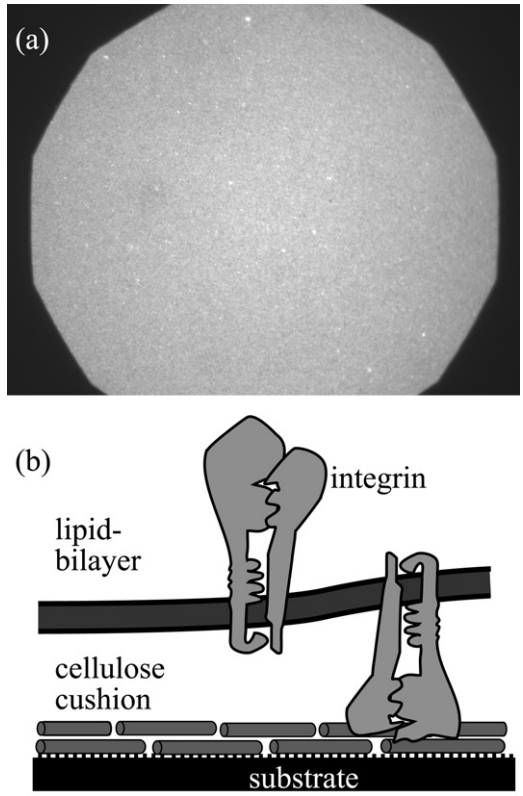

FIGURE 3 (*a*) Fluorescence micrograph of an integrin-doped membrane on a cellulose film. (*b*) Schematic drawing of the polymer cushioned membrane viewed from the side.

The fluorescence distribution (and thus the protein distribution) is heterogeneous and numerous dark patches are visible, showing that the coverage is incomplete. These heterogeneous patches and defects could not be healed out, even after prolonged incubation. This finding is in contrast to the homogeneous membrane reported by (Erb et al., 1997), although the preparation procedures are very similar. However, as shown in Fig. 3 and as more clearly demonstrated by lateral diffusion measurements (cf. following section) a perfectly homogeneous and fluid membrane is formed by spreading of vesicles on a cellulose ''cushion.''

Determination of lateral diffusion constants

FRAP experiments were carried out to determine the lateral diffusion constant D and the mobile fraction of integrin receptors and lipids in the two types of supported membranes. To eliminate effects of drift of the optical paths, the quality of the focus (in lateral and horizontal plane) was checked after each measurement. For the membrane on bare glass slides, no fluorescence recovery could be observed during the observation time (cf. *gray circles* in Fig. 4 *a*). The same qualitative result is obtained for a membrane on a quartz substrate (data not shown). In the case of membranes supported on polymer cushions, however, we obtain a recovery of the fluorescence signal of $R = 25 \pm 5\%$ (*black squares* in Fig. 4 *a*). Analysis of the recovery curve yielded a diffusion constant of $D = 0.6 \pm 0.2\ \mu m^2\ s^{-1}$. To understand the origin of the low recovery, we performed two subsequent bleaching experiments at the same position of the sample. The recovery curve of the second bleaching experiment is shown in Fig. 4 *b*. A comparison of the black curves in Fig. 4 *a* and 4 *b* shows that the fraction of fluorescence recovery increased drastically in the second bleaching experiment. Since all immobile proteins are irreversibly bleached during the first laser pulse, only mobile fluorescent proteins can diffuse into the bleached spot and contribute to the fluorescence signal in the second experiment. Thus only mobile integrins are observed and we therefore obtain a higher recovery rate of $86 \pm 5\%$, whereas the diffusion constant D is the same as before. These findings strongly suggest that mobile and immobile integrin species coexist in the membrane. It is reasonable to assume that all receptors with the large headgroups facing toward the substrate are immobile. According to previous electron microscopy studies the two orientations of the receptors are evenly distributed in the original vesicle preparation. One would thus expect that 50% of the receptors should be fully mobile and fully functional. The immobilization of proteins with the large extracellular domain pointing to the aqueous phase could be due 1), to local clustering of receptors within the

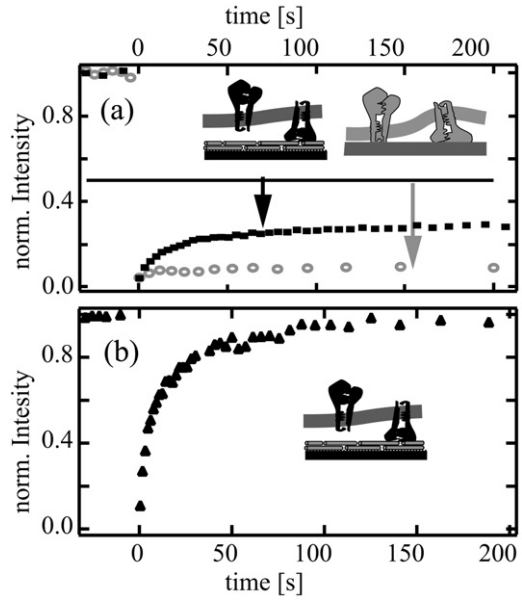

FIGURE 4 (*a*) Fluorescence recovery after photobleaching (FRAP) curves of supported membranes containing labeled integrin. The gray circles correspond to the fluorescence signals from a membrane deposited directly on a bare glass substrate, whereas the black squares indicate the recovery curve of a membrane supported on a cellulose film (as depicted in the *insets*). For the membrane on the polymer cushion the percentage of fluorescence recovery is 25%. (*b*) The recovery curve obtained after another bleaching pulse applied to the same sample position. The recovery attains 86%.

supported membrane 2), to nonspecific attraction between the proteins and the cellulose films, or 3), to nonspecific binding to defects in the cellulose film.

The existence of defects in the supported membranes is suggested by measurements of the lipid diffusion. For these experiments the fluorescent lipid NBD-PC was added to the integrin-containing membrane. We obtained a diffusion constant $D = 3.3 \pm 0.2\ \mu m^2\ s^{-1}$ and a recovery fraction of $77 \pm 1\%$ for the membrane on cellulose cushions. Bleaching again the same spot yielded a higher mobile fraction of $96.9 \pm 0.1\%$ while the diffusion constant D remained the same. This result shows that the supported membrane on the polymer cushion exhibits still a remarkable density of defects, which could comprise an area fraction of ~20%. Receptors in this area fraction are expected to be immobile.

The measured lipid diffusion constants are a factor of three larger than those reported for pure lipid bilayers on polymer supports or bare glass substrates (Sigl et al., 1997). This can be interpreted in terms of the reduced frictional coupling between the membrane and the surface, which is inversely proportional to the thickness of the water layer in between (Evans and Sackmann, 1988). The rather rigid protein headgroups are expected to act as spacers between the polymer cushion and the lipid bilayer, hence friction between lipids and the polymer film is expected to be smaller. The value of $D = 3.3 \pm 0.2\ \mu m^2\ s^{-1}$ is about half of the lipid diffusivity in a free bilayer membrane of pure DMPC (Almeida et al., 1992).

Interestingly, the diffusion constant of the lipids in the supported membranes on bare glass slides is a factor of 10 smaller than in polymer supported membranes. This could be explained by assuming that the integrins adsorbing with their large extracellular domain on the surface can hinder the diffusion of lipids drastically (Chan et al., 1991, Kucik et al., 1999). Another explanation is that the diameter of the bleaching pulse (9.3 μm) is larger than the size of most of the continuous lipid patches, which would result in a reduced long-range diffusion coefficient.

Functionality test of integrin

The functionality of the reconstituted receptors in supported membranes was evaluated by quantitative analysis of the specific binding to a cyclic hexapeptide containing the RGD sequence, which is specifically recognized by the $\alpha_{IIb}\beta_3$ receptor. Two series of binding tests were adopted: firstly, the binding of fluorescently labeled RGD peptides to supported membranes was tested. The fluorescence intensity in the presence of integrin (cf. Fig. 5) was a factor of two

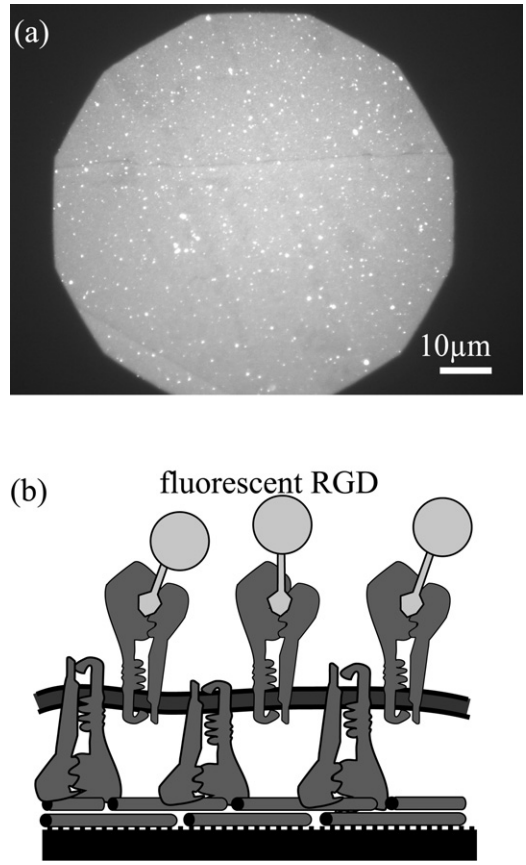

FIGURE 5 (*a*) Fluorescence micrograph of the labeled RGD peptides bound to integrin-doped membrane supported on a cellulose cushion. (*b*) Schematic presentation of the side view of the membrane, where synthetic ligands bind only to the integrins pointing their extracellular headgroup into the aqueous phase.

higher than in the absence of receptors in the membrane. Another clear difference between the two samples appeared when the dyes were continuously illuminated. For the membrane with integrin, we observed a continuous bleaching of fluorescent dyes, as manifested by an exponential decay of the signal intensity. In contrast, for pure membranes the fluorescence from the labeled RGD peptides remained constant, suggesting that in this case the fluorescence signal comes from RGD peptides in the bulk solution.

The second and more powerful test of the functionality is based on the study of adhesion of giant vesicles bearing RGD lipids by using RICM. A typical RICM image of a giant vesicle with RGD lipids adhering to an integrin-containing bilayer on a cellulose film is shown in Fig. 6 *a*. Strong adhesion is indicated by the formation of a dark disc, where the distance between membrane and substrate is smaller than 30 nm (Bruinsma et al., 2000). The picture shown was obtained by averaging over 20 subsequent images (~1 s). The interferogram exhibits well-defined Newton rings, indicating that the vesicle is not moving or does not show strong thermally excited bending fluctuations. This is a consequence of the strong adhesion which leads to the suppression of the membrane flickering by the adhesion induced membrane tension (Albertsdörfer et al., 1997).

In contrast, RGD lipid and PEG lipid containing giant vesicles in contact with pure supported DMPC membranes do not adhere. No dark adhesion plaques are observed. The same is found for pure giant DMPC vesicles in contact with an integrin-containing supported membrane. Thus, strong adhesion of vesicles does not take place in the absence of either the receptors integrin $\alpha_{IIb}\beta_3$ or the conjugated ligands (RGD lipids).

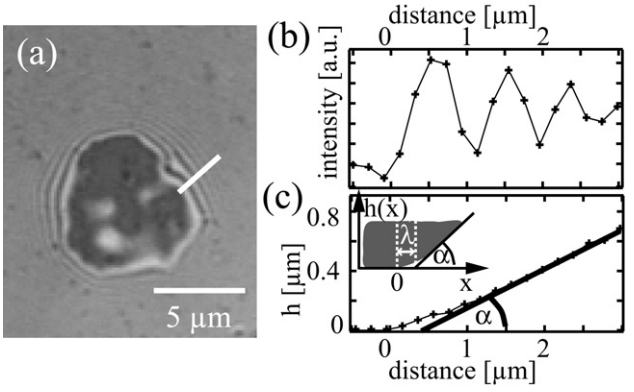

FIGURE 6 (*a*) Reflection interference contrast microscopy (RICM) image of a giant vesicle containing 1% RGD lipid and 2% PEG lipid adhering to a membrane with integrin $\alpha_{IIb}\beta_3$. The membrane is supported by a cellulose cushion. The dark areas indicate strongly adhered patches. Newton fringes around the contact area show lines of equal height of the membrane above the surface. (*b*) Intensity profile along the straight line indicated in the interferogram. (*c*) The local height profile shown is reconstructed from the intensity profile. The contact angle α and the characteristic capillary length λ are defined in the height profile. The zero point of the x axis ($x = 0$) is determined by the onset of the upward deflection of the membrane from the substrate.

Adhesion strength on bare glass and on cellulose films

It is interesting to compare the adhesion strength of vesicles adhering on the membrane deposited onto bare glass and onto cellulose films, since this will yield insights into the effects of the mobility and functionality of receptors on the adhesion. In Fig. 6 *a*, an adhering vesicle on an integrin-containing membrane supported by a cellulose cushion is shown. Fig. 7 *a* shows a vesicle in contact with a bilayer supported directly on bare glass. The adhesion in the latter case is weaker, because only a small part of the contact area adheres strongly as indicated by dark patches (cf. *arrows* in Fig. 7). Most of the adhesion disc consist of large bright areas, which correspond to weak adhesion. The blurred appearance of the vesicle in Fig. 7 *b* indicates that the contact area fluctuates strongly.

The free energy of adhesion Δg_{ad} per unit area (also called spreading pressure) of the vesicle to the substrate can be determined by two different methods:

1. One way is to analyze the contour of the vesicle in terms of mechanical equilibrium at the contact line of the adhering vesicle with the substrate. This is described by the classical wetting equation of Young-Dupré (Evans, 1974, Bell et al., 1984, Bruinsma et al., 2000):

$$\Delta g_{ad} = \gamma(1 - \cos\alpha), \tag{1}$$

where α is the contact angle defined in Fig. 6, *c* and γ the lateral membrane tension (corresponding to the surface tension of a liquid). This equation holds for fluid membranes, when the tension of the vesicle membrane is homogeneous.

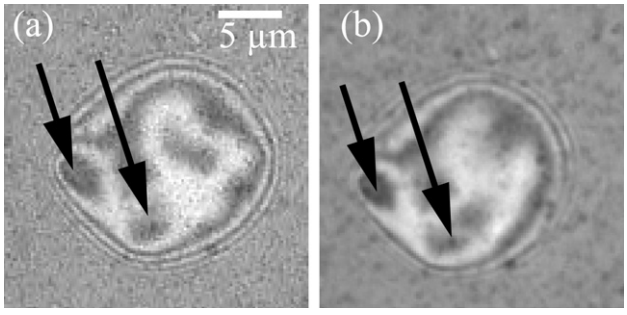

FIGURE 7 (*a*) RICM interferogram of a giant vesicle with 1% RGD lipid and 2% PEG lipid adhering to an integrin-doped membrane on a bare glass substrate (integration time 59 ms). The arrows indicate the strongly adhering (*dark*) area, whereas the main area of the adhesion disc adheres only weakly (*light areas*) and exhibits strong flickering. (*b*) RICM image of the same giant vesicle taken with a prolonged integration time of 5 s. Due to the motion of the contact area, the vesicle exhibits a bleary appearance.

2. The second method is based on the analysis of the vesicle global shape as a function of the vesicle membrane area to the vesicle volume (called the degree of deflation) following Seifert and Lipowsky (1990). By respecting the equilibrium of the bending moments of the membrane near the surface this approach predicts:

$$2\Delta g_{ad} = \frac{\kappa}{R_C^2}, \tag{2}$$

where κ is the bending stiffness and R_C is the contact curvature. The geometric parameter R_C is the curvature at the transition from the adhering to the nonadhering regions of the vesicle.

Unfortunately, the contact curvature is difficult to measure. Therefore, a more accurate method to determine Δg_{ad} is based on a model suggested by Bruinsma (1995). The following equation for the height profile of the membrane in the vicinity of the contact line is obtained:

$$h(x) = \alpha(x - \lambda) + \alpha\lambda \exp\left(-\frac{x}{\lambda}\right), \tag{3}$$

where x is defined in Fig. 6 *c*, α is the macroscopic contact angle between the membrane and the substrate, and $\lambda = \sqrt{\kappa/\gamma}$ is the capillary length. λ is a measure for the length over which the deformation of the membrane at the contact line is determined by the local bending deformation. Thus, for $x > \lambda$ the vesicle shape is tension dominated. It is easily verified that λ is related to the contact curvature according to $\lambda = \alpha R_C$, as the second derivative of Eq. 3 at $x = 0$ is the inverse contact curvature R_C. The geometric parameters α and λ can be determined from the RICM image for each location along the rim of the adhesion disc (Albertsdörfer et al., 1997).

The capillary length λ is determined by the distance between $x = 0$ and the intersection of the straight line fitted to the contour of the vesicle for $x \gg \lambda$ and the x axis. The zero point of the axis ($x = 0$) is determined by the onset of the deflection of the membrane (cf. Fig. 6 *c*). The bending stiffness κ is assumed to be 100 k_BT for the DMPC vesicle containing 50 mol % cholesterol. According to the Young equation (Eq. 1), the local adhesion energy Δg_{ad} could in principle be determined at every position of the rim. However, since the values of λ can not be easily determined for regions of tight adhesion, more accurate results are obtained by measuring the tension γ at sites of weak adhesion, which exhibit many Newton rings. Then, owing the isotropic tension, this value of γ is used to determine the adhesion energies Δg_{ad} at tight adhesion domains according to Eq. 1. In Fig. 8 we show an example of the distribution of the contact angles α and free adhesion energy densities Δg_{ad} for a vesicle containing 2% PEG lipid adhering to a cellulose supported bilayer. At site numbers 0 and 9, the capillary length as well as the contact angle can be measured with high accuracy, whereas in the domains of tight adhesion (site numbers 3 and 6) only the contact angle can be measured reliably. The free adhesion energies per unit area measured for a given set of concentrations (c_R, c_{Li}) at various sites of the adhesion disc, agree remarkably well (cf. Fig. 8). This shows that the vesicle is in thermodynamic equilibrium which is an important condition to obtain reproducible results. The free adhesion energy Δg_{ad} obtained for different concentrations of repeller molecules and 1% RGD lipid onto different substrates are presented in the histogram in Fig. 9.

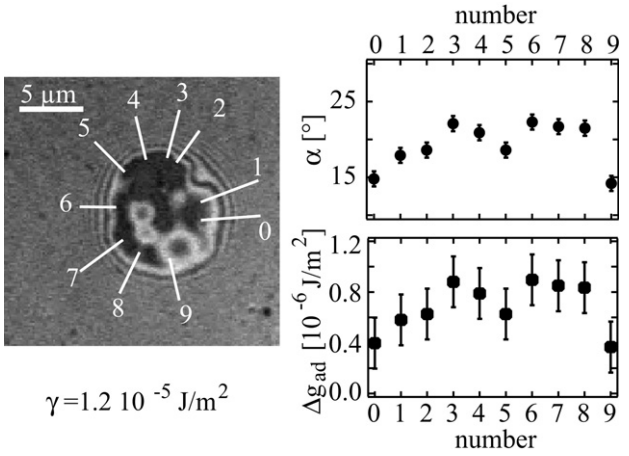

FIGURE 8 Measurement of membrane tension γ, contact angle α (*circles*) and free adhesion energy densities Δg_{ad} (*squares*) at sites of strong (*black regions*) and weak (*light regions*) adhesion near the rim of the adhesion disc.

Estimation of the specific adhesion energy W_{ad}

In the following, we attempt to compare the measured values of Δg_{ad} for strong adhesion sites with the specific adhesion energy W_{ad} (cf. Eq. 4, below), estimated as follows. By

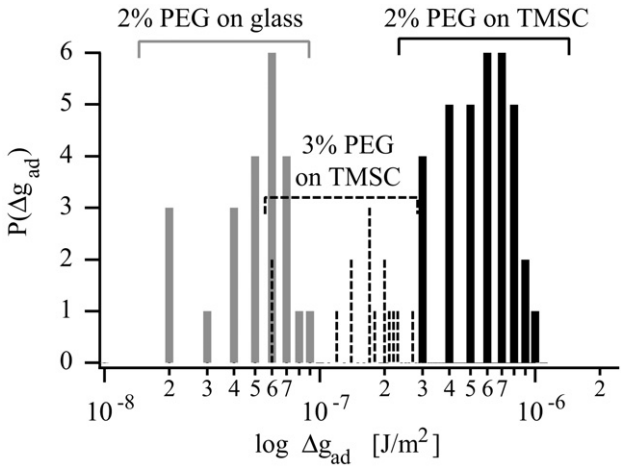

FIGURE 9 Histograms of measured values of free energies of adhesion of vesicles containing 2 and 3 mol % of repeller lipids (PEG lipids) on cellulose (*black* and *dotted lines*, respectively) and of vesicles containing 2 mol % PEG lipids on bare glass substrates (*gray lines*). Note that the largest value correspond to regions of tight adhesion, whereas the lowest values correspond to the spreading pressures of the regions of weak adhesion.

assuming firstly that the integrin concentration within the strong adhesion plaque is about equal to the initial concentration and secondly that 50% of the integrins exhibit the functional headgroup toward the aqueous phase, the integrin receptor density is $n_I \approx 7 \times 10^{13}\ m^{-2}$. The binding energy of the receptor-ligand pair has not been measured yet, but it can be estimated from the dissociation constant of the hexapeptide-integrin pair, $k_{D(I\text{-}RGD)} \approx 1.1 \times 10^{-6}$ M (Hu et al., 2000). This k_D value is a factor of 10^9 smaller than the corresponding value reported for the biotin-streptavidin bond ($k_{D(B\text{-}S)} \sim 10^{-15}$ M), which has a binding energy of $w_{ad(B\text{-}S)} \sim 35\ k_BT$ (Bayer, 1990). This approach yields $w_{ad(I\text{-}RGD)} \sim 10\ k_BT$ for the integrin-RGD binding energy. Note that this is a lower limit of the binding energy since the density of receptors n_I would be a factor of two smaller if the immobilized fraction of receptors is not functional.

The specific adhesion energy in our experiments is then expected to be in the order of $W_{ad} \approx n_I \times w_{ad(I\text{-}RGD)} \approx 3 \times 10^{-6}\ J\ m^{-2}$. According to Fig. 9, this value is only 3 and 10 times larger than the largest spreading pressure Δg_{ad} found for vesicles containing 2% and 3% PEG lipids, respectively. It is 30 times larger than the largest value of Δg_{ad} found for vesicles containing 2% PEG lipid on pure glass substrates (cf. Fig. 9).

The relatively small discrepancies between the values of W_{ad} and Δg_{ad} for the cellulose covered substrates can be understood as follows (Sackmann and Bruinsma, 2002). The free adhesion energy has been shown to depend not only sensitively on the receptor and ligand densities and their binding energy, but also on the repeller concentration c_R since the two-dimensional osmotic pressure difference between the adhesion plaque and the nonadherent membrane regions reduces the free energy of adhesion drastically (Bell et al., 1984, Bruinsma et al., 2000). By ignoring effects of the membrane elasticity, the free energy of adhesion can be expressed as

$$\Delta g_{ad} = W_{ad} - \Delta\pi_R - \Delta\pi_{Li}, \tag{4}$$

where $\Delta\pi_R$ and $\Delta\pi_{Li}$ is the osmotic pressure difference of the repellers and ligands, respectively. W_{ad} is the specific adhesion energy per unit area of the receptor-ligand pairs. The osmotic pressure difference $\Delta\pi_R$ arises since the repeller molecules are partially expelled from the tight adhesion domains due to the steric repulsion generated by the large PEG headgroups having a Flory radius $R_F \simeq 3$ nm (de-Gennes, 1980). Because the headgroups of the RGD ligands are very small, they are expected to be rather evenly distributed between strongly adhering regions and the free membrane and their effect is thus ignored in the following. The osmotic pressure difference of the repellers can be estimated from van't Hoff's law:

$$\Delta\pi_R = k_BT\Delta c_R, \tag{5}$$

where Δc_R is the difference in the repeller concentration between the adherent and free membrane regions.

If the local repeller concentration in the adhesion domain is assumed to be zero and the area per lipid is 100 Å^2, the osmotic pressure (for 2 mol % PEG lipid) would be $\Delta\pi_R \approx 8 \times 10^{-5}\ J\ m^{-2}$ (according to Eq. 5). This value is much higher than the measured spreading pressure ($\Delta g_{ad} = 1 \times 10^{-6}\ J\ m^{-2}$, cf. Fig. 9). In order to account for the difference between the spreading pressure Δg_{ad} and the estimated specific interaction energy W_{ad}, we calculate the energetic difference to $2 \times 10^{-6}\ J\ m^{-2}$ for the case of 2% PEG by application of Eq. 4. The concentration difference Δc_R necessary to generate this difference is determined to $\Delta c_R \sim 0.03 c_R$, which is very small. The existence of a rather high density of PEG lipids in the tight adhesion plaques suggested here, can be explained in terms of the larger integrin head groups (~12 nm) than the Flory radius of the PEG lipid ($R_{Flory} \approx 3$ nm).

According to Eq. 4, the specific adhesion energy W_{ad} is obtained from the measurement of Δg_{ad} by extrapolation Δg_{ad} versus the PEG lipid concentration c_R to $c_R = 0$. This approach yields a free adhesion energy $\Delta g_{ad(cR\,=\,0)} = 2 \times 10^{-6}\ J\ m^{-2}$ at $c_R = 0$. This extrapolated value of Δg_{ad} agrees well with the predicted specific adhesion energy in the tight adhesion plaques $W_{ad} = 3 \times 10^{-6}\ J\ m^{-2}$. We can conclude further that the mobile integrin receptors do not accumulate remarkably in the tight adhesion domains. A possible explanation of this finding is that the accumulation of the receptors is impeded by the presence of repeller molecules.

The much smaller value of the free adhesion energy Δg_{ad} on an integrin-doped membrane supported by a bare glass surface (cf. Fig. 9), can be attributed to the partial denaturation of the receptors, since effects of the osmotic pressure difference should be similar to that in the vesicle on polymer-supported membranes.

CONCLUSIONS

To design models of cell surfaces, we established solid supported membranes with incorporated, large transmembrane proteins, such as integrin receptors. The membranes were separated from the solid substrates by ultrathin, soft cellulose multilayers. These polymer cushions were shown to be particularly well suited as biocompatible soft surface to prepare macroscopically homogeneous supported membranes. A fraction of 25% of the integrin receptors on the cellulose cushion exhibits long range lateral mobility (diffusion constant $D = 0.6\ \mu m^2\ s^{-1}$), attributed to the proteins pointing their large headgroups into the aqueous phase. Integrins incorporated in membranes supported on bare glass substrates are essentially immobilized. Additionally, a drastic reduction in the adhesion strength of the receptors on these surfaces was observed, in comparison to the adhesion strength on soft polymer surfaces. The free adhesion energy (spreading pressure) Δg_{ad} could be measured quantitatively in terms of the elastic boundary conditions. It corresponds to the difference of the specific energy W_{ad} and the lateral

osmotic pressure exerted by the repeller molecules $\Delta\pi_R$. Previously, it was reported that the adhesion process is accompanied by repeller segregation and adhesion plaque formation. The results here however show, that the repeller concentration in the adhesion plaque is only about 3% smaller than that in the free membrane. Because the Flory radius of the used repeller (3 nm) is smaller than the receptor headgroup (12 nm), the repeller depletion, enforced by the interplay of short range attraction of receptor-ligand pairs and the long-range generic repulsion, is weak for the present system.

Measurements of Δg_{ad} as a function of the repeller concentration allowed us to estimate the specific adhesion energy W_{ad} of the vesicle to the substrate. By neglecting receptor condensation, we obtain for the specific receptor-ligand binding energy a lower limit $w_{ad(1-RGD)} \simeq 10\,k_BT$. An independent measurement of the local receptor density in the adhesion plaque would be necessary for a more reliable determination of an absolute value of w_{ad}. However, the present technique provides a simple and powerful tool to measure relative values of the receptor-ligand binding energies of different receptor-ligand pairs under the bioanalogue condition that both interacting surfaces are fluid. The strong reduction of the binding energy observed for membranes supported by bare glass shows the importance of depositing membranes on soft polymer films for quantitative adhesion studies.

We thank M. Rusp for the preparation of the integrin vesicles, Dr. S. Kaufmann for the help with the phosphate analysis and protein concentration measurements, and Dr. M. Bärmann for helpful advice in biochemistry. F. Foerster from the MPI für Biochemie in Martinsried took the electron microscopy image. K. Behrendt is acknowledged for the fluorescent labeled RGD peptide and J. Schilling for developing the real time imaging software. O. Purrucker is acknowledged for a critical reading of the manuscript. One of the authors (M.T.) is grateful to Prof. G. Wegner for helpful suggestions in cellulose chemistry.

This work was supported by the Deutsche Forschungs Gesellschaft (SFB 563) and the Fonds der Chemischen Industrie. M.T. is thankful to DFG for Habilitation fellowship (Emmy Noether-Program).

REFERENCES

Albertsdörfer, A., T. Feder, and E. Sackmann. 1997. Adhesion-induced domain formation by interplay of long-range repulsion and short-range attraction force: A model membrane study. *Biophys. J.* 73:245–257.

Almeida, P., W. Vaz, and T. Thompson. 1992. Lateral diffusion in the liquid phase of dimyristoylphosphatidylcholine/cholesterol lipid bilayers: A free volume analysis. *Proc. Natl. Acad. Sci. USA.* 79:5171–5174.

Axelrod, D., D. Koppel, J. Schlessinger, E. Elson, and W. Webb. 1976. Mobility measurements by analysis of fluorescence photobleaching recovery kinetics. *Biophys. J.* 16:1055–1069.

Bayer, E. 1990. Avidin-Biotin Technology, Vol. 184 of Methods in Enzymology, Academic Press, Inc.

Bell, G., M. Dembo, and P. Bongrand. 1984. Competition between nonspecific repulsion and specific bonding. *Biophys. J.* 45:1051–1064.

Bradford, M. 1976. A rapid and sensitive method for the quantitation of microgram quantities of protein utilizing the principle of protein-dye binding. *Anal. Biochem.* 72:248–254.

Brian, A. A., and H. M. McConnell. 1984. Allogenic stimulation of cytotoxic T-cells by supported planar membranes. *Proc. Natl. Acad. Sci. USA.* 81:6159–6163.

Bruinsma, R. 1995. Adhesion and Rolling of Leukocytes. A Physical Model. Proceedings of the NATO Advanced Institute of Physics and Biomaterials., NATO Advanced Study Institute Series B: Physics, Kluwer, p. 611.

Bruinsma, R., A. Behrisch, and E. Sackmann. 2000. Adhesive switching of membranes: experiment and theory. *Phys. Rev. E.* 61:4253–4267.

Chan, P., M. Lawrence, M. Dustin, L. Ferguson, D. Golan, and T. Springer. 1991. Influence of receptor lateral mobility on adhesion strengthening between membranes containing LFA-3 and CD2. *J. Cell Biol.* 115:245–255.

deGennes, P. 1980. Conformations of polymers attached to an interface. *Macromolecules.* 13:1069–1075.

Dimitrov, D., and M. Angelova. 1988. Lipid swelling and liposome formation mediated by electric fields. *Bioelectrochem. Bioenerg.* 19:323–336.

Dustin, M. 1997. Adhesive bond dynamics in contacts between T lymphocytes and glass-supported planar bilayers reconstituted with the immunoglobulin related adhesion molecule CD58. *J. Biol. Chem.* 272:15782–15788.

Erb, E., K. Tangemann, B. Bohrmann, B. Müller, and J. Engel. 1997. Integrin alpha IIb beta 3 reconstituted into lipid bilayers is nonclustered in its activated state but clusters after fibrinogen binding. *Biochemistry.* 36:7395–7402.

Evans, E. 1974. Bending resistance and chemically-induced moments in membrane bilayers. *Biophys. J.* 14:923–931.

Evans, E., and E. Sackmann. 1988. Translational and rotational drag coefficients for a disk moving in a liquid membrane associated with a rigid substrate. *J. Fluid. Mech.* 194:553–561.

Fiske, C., and Y. SubbaRow. 1925. The colorimetric determination of phosphorus. *J. Biol. Chem.* 66:375–400.

Fitzgerald, L., B. Leung, and D. Phillips. 1985. A method for purifying the platelet membrane glycoprotein IIB-IIIA complex. *Anal. Biochem.* 151:169–177.

Gurrath, M., G. Müller, H. Kessler, M. Aumailley, and R. Timpl. 1992. Conformation/activity studies of rationally designed potent anti-adhesive RGD peptides. *Eur. J. Biochem.* 210:911–921.

Heyse, S., H. Vogel, M. Sänger, and H. Sigrist. 1995. Covalent attachment of functionalized lipid bilayers to planar waveguides for measuring protein binding to biomimetic membranes. *Protein Sci.* 4:2532–2544.

Hillebrandt, H., G. Wiegand, M. Tanaka, and E. Sackmann. 1999. High electric resistance thin polymer/lipid composite systems on indium-tin-oxide (ITO) electrode-arrays. *Langmuir.* 15:8451–8459.

Hu, B., D. Finsinger, K. Peter, Z. Guttenberg, M. Bärmann, H. Kessler, A. Escherisch, L. Moroder, J. Böhm, W. Baumeister, S. Sui, and E. Sackmann. 2000. Intervesicle cross-linking with integrin alpha(IIb)beta(3) and cyclic-RGD-lipopeptide. A model of cell-adhesion processes. *Biochemistry.* 39:12284–12294.

Hynes, R. 1992. Integrins: Versatility, modulation, and signaling in cell adhesion. *Cell.* 69:11–25.

Kalb, E., S. Frey, and L. Tamm. 1992. Formation of supported planar bilayers by fusion of vesicles to supported phospholipid monolayers. *Biochim. Biophys. Acta.* 1103:307–316.

Kucik, D., E. Elson, and M. Scheetz. 1999. Weak dependence of mobility of membrane protein aggregates on aggregate size supports a viscous model of retardation of diffusion. *Biophys. J.* 76:314–322.

Mooney, J. F., A. J. Hunt, J. R. McIntosh, C. A. Liberko, D. M. Walba, and C. T. Rogers. 1996. Patterning of functional antibodies and other proteins by photolithography of silane monolayers. *Proc. Natl. Acad. Sci. USA.* 93:12287–12291.

Müller, B., H. Zerwes, K. Tangemann, J. Peter, and J. Engel. 1993. 2-step binding mechanism of fibrinogen to alpha IIb beta 3 integrin reconstituted into planar lipid bilayers. *J. Biol. Chem.* 268:6800–6808.

Puu, G., E. Artursson, I. Gustafson, M. Lundström, and J. Jass. 2000. Distribution and stability of membrane proteins in lipid membranes on solid supports. *Biosens. Bioelectron.* 15:31–41.

Sackmann, E. 1996. Supported membranes: Scientific and practical applications. *Science*. 271:43–48.

Sackmann, E., and R. Bruinsma. 2002. Cell adhesion as wetting transition? *Chem Phys Chem.* 3:262–269.

Salafsky, J., J. Groves, and S. Boxer. 1996. Architecture and function of membrane proteins in planar supported bilayers: A study with photosynthetic reaction centers. *Biochemistry*. 35:14773–14781.

Schaub, M., G. Wenz, G. Wegner, A. Stein, and D. Klemm. 1993. Ultrathin films of cellulose on silicon wafers. *Advanced Materials.* 5:919–922.

Seifert, U., and R. Lipowsky. 1990. Adhesion of vesicles. *Phys. Rev. A.* 42:4768–4771.

Sigl, H., G. Brink, M. Schulze, G. Wegener, and E. Sackmann. 1997. Assembly of polymer/lipid composite films on solids based on hairy rod LB-films. *Eur. Biophys. J.* 25:249–259.

Soumpasis, D. 1983. Theoretical analysis of fluorescence photobleaching recovery experiments. *Biophys. J.* 41:95–97.

Tanaka, M., S. Kaufmann, J. Nissen, and M. Hochrein. 2001. Orientation selective immobilization of human erythrocyte membranes on ultrathin cellulose films. *Phys. Chem. Chem. Phys.* 3:4091–4095.

Watts, T., H. Gaub, and H. McConnell. 1986. T-cell-mediated association of peptide antigen and major histocompatibility complex protein detected by energy transfer in an evanescent field. *Nature*. 320:179–181.

Wegner, G. 1993. Control of molecular and supramolecular architecture of polymer, polymer systems and nanocomposites. *Mol. Cryst. Liq. Cryst.* 235:1–34.

Wong, J., C. Park, M. Seitz, and J. Israelachvili. 1999. Polymer-cushioned bilayers. II. an investigation of interaction forces and fusion using the surface forces apparatus. *Biophys. J.* 77:1458–1468.